Supporting Information

Green synthesis of open porous NiO films with excellent capacitance performance

Yabin Zhang[ab] and Zhiguang Guo *[ab]

[a] Ministry of Education Key Laboratory for the Green Preparation and Application of Functional Materials, Hubei University, Wuhan 430062, People's Republic of China. E-mail: zguo@licp.cas.cn

[b] State Key Laboratory of Solid Lubrication, Lanzhou Institute of Chemical Physics, Chinese Academy of Sciences, Lanzhou 73000, China

Experimental section

Preparation of open porous NiO films on ITO/glass substrate: All the chemical reagents were analytical grade and used as received without further purification. $Ni(NO_3)_2 \cdot 6H_2O$ (5 mmol, 1.4541 g) was dissolved in deionized water (25 mL) and ethylene glycol (25 mL) to form a clear light green solution under constant magnetic stirring. Subsequently, glucose (0.01 g, 0.050 mmol) was added into the solution and continue to stir for another 30 min. The ITO substrate (about 2 cm×2.5 cm) was carefully cleaned by ultralsonication sequentially in acetone, isopropanol, deionized water, and ethanol for 20 min each. Then the mass of the substrate was recorded after being dried with N_2 flow. Next, the substrate was placed obliquely into a polytetrafluoroethylene (PTFE) (Teflon)-lined autoclave with the conductive side facing downward. The aqueous solution was transferred into autoclave and maintained at 160 ° C for 24 h, and allowed to cool down to room temperature naturally. The light green substrate was washed with deionized water and ethanol 5 times each, and dried in an oven at 60 ° C for 14 h. The deposited NiO films on back (non-conductive) side were removed with water flow during the washing process or erased with filter paper after dryness. Finally, the samples were annealed in a muffle furnace at 350 ° C for 3 h in air, and were ready for structural characterization. Before electrochemical tests, the real area of NiO film on ITO/glass was fixed to 2 cm×2 cm through erasing the redundant part with filter paper, and the weight of this NiO-on-ITO sample was recorded (Figure S1b). Consequently, the mass of active materials on ITO/glass was obtained by subtracting the mass of the original ITO/glass substrate from the as-measured mass of NiO-on-ITO sample. The masses of all the as-obtained samples were calculated by the above method, which range from 0.3 mg to 0.6 mg.

Characterizations: The crystal structure of the as-prepared samples were characterized by X-ray diffraction (XRD) analysis using a X'SPERT PRO diffractmeter with Cu Kα radiation of 1.5418 Å

wavelength at 2θ ranging from 5° to 80°. The surface morphologies of the as-prepared samples were observed by a JSM-5600LV scanning electron microscope (SEM), operated at 20.0 kV. Transmission electron microscope (TEM) images and the corresponding selected-area electron diffraction (SAED) pattern were captured on a FEI Tecnai G 20 TEM at an acceleration voltage of 200.0 kV. High resolution transmission electron microscope (HRTEM) images were taken using a JEM-1200EX TEM with an accelerating voltage of 200 kV.

Electrochemical tests: The electrochemical tests were carried out in a CH660D (Chenhua, China) electrochemical workstation using a three-electrode system containing 1 M KOH electrolyte solution at room temperature. Mercuric oxide electrode (Hg/HgO) and platinum were used as the reference and counter electrodes, respectively. The masses of the sample used for electrochemical tests is 0.4 mg, which is evaluated by the above method.

Cyclic voltammetry (CV) tests were performed between 0-0.5V (vs. Hg/HgO) potential window at scan rates of 10, 20, 30, 40, 50 and 60 mV/s. The electrochemical impedance spectroscopy (EIS) measurements were carried out in the frequency range from 0.01 Hz to 100 kHz at an open-circuit potential with an ac perturbation of 5 mV. The galvanostatic charge-discharge (chronopotentiometry) measurements were performed at current density of 1, 2, 4, 8, 16 and 20 A/g.

Material	Charge storage mechanism	Specific capacitance	Rate capability	Cycling stability	Reference
NiO	$NiO+OH^-=NiOOH+e^-$	1153~960 F/g (1~20 A/g)	83.3%	93.1% at 8 A/g for 5000	our work
$Ni(OH)_2$	$Ni(OH)_2+OH^-=NiOOH+H_2O+e^-$	2222~1103 F/g (1~30 A/g)	77.3%	76.3% at 10 A/g for 2000	ref. 1
Co_3O_4	$Co_3O_4+OH^-+H_2O=3CoOOH+e^-$ $CoOOH+OH^-=CoO_2+H2O+e^-$	2735~147 F/g (2~10 A/g)	53.8%	94.2% at 8 A/g for 2000	ref. 2
$Co(OH)_2$	$Co(OH)_2+OH^-=CoOOH+H_2O+e^-$ $CoOOH+OH^-=CoO_2+H_2O+e^-$	1473~987 F/g (2~32 A/g)	67%	88% at 6 A/g for 1000	ref. 3
MnO_2	$MnO_2+M^++e^-=MMnO_2$ (M could be H^+, Li^+, Na^+, K^+)	201~96 F/g (1~20 A/g)	47.8%	65% at 5 A/g for 1800	ref. 4
CuO	$2CuO+2A^++2e^-=CuOOA$ $(2CuO)_{surface}+2A^++2e^-=2(CuOOA)_{surface}$ (A could be H^+, Na^+)	346~222 F/g (5~100 mV/s)	64.2%	$ca.$78% at 100 mV/s for 2000	ref. 5
V_2O_5	$V_2O_5+2M^++2e^-=M_2V_2O_5$ (M could be H^+, Li^+, Na^+, K^+)	451~150 F/g (0.5~50 A/g)	33.3%	90% at 5 A/g for 1800	ref. 6

Table S1 Capacitance performance of 2D transition-metal oxide/hydroxide electrodes

Materials	Rate capability		Capacitance retention (%)	
Mesoporous NiO[7]	50%	from 2 A/g to 20 A/g	90%	at 2 A/g for 1000
Nano-structured NiO[8]	70%	from 2A/g to 40 A/g	70%	at 40 A/g for 1000
Hierarchical NiO hollow sphere[9]	80%	from 0.5 A/g to 3 A/g	91%	at 3 A/g for 1000
Hierarchical NiO hollow nanostructure[10]	41.9%	from 1.5 A/g to 20 A/g	87.5%	at 6 A/g for 1000
Flowerlike NiO hollow nanosphere[11]	41.6%	from 2 A/g to 10 A/g	95%	at 5 A/g for 1000
NiO macrotubes[12]	86.5%	from 0.5 A/g to 3 A/g	93%	at 1.5 A/g for 1000
Hierarchical NiO nanospheres[13]	77%	from 0.5 A/g to 4.5 A/g	95%	at 0.5 A/g for 1000
Porous nickel oxide microflowers[14]	51%	from 0.625 A/g to 6.25 A/g	99.7%	at 6.25 A/g for 1000
Porous NiO nanosheets[15]	31.8%	from 3 A/g to 15 A/g	98.2%	at 15 A/g for 500
Hierarchical NiO[16]	74%	from 1 A/g to 4 A/g	98%	at 4 A/g for 1700
NiO nanobelts[17]	25.2%	from 2 A/g to 10 A/g	95%	at 5 A/g for 2000
Porous NiO nanowall arrays[18]	87.4%	from 0.67 A/g to 13.35 A/g	93%	at 1.6 A/g for 4000
Hexagonal NiO nanoplatelet arrays[19]	77%	from 2 A/g to 16 A/g	92%	at 8 A/g for 5000
NiO ultrathin nanowire networks[20]	70%	from 2 A/g to 10 A/g	97%	at 10 A/g for 2000

Table S2 Rate performance and cycling stability of the as-reported various NiO-based electrode for pseudo-capacitance.
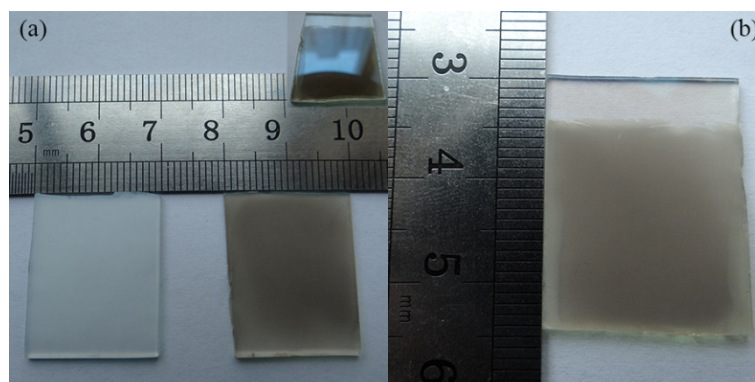

Figure S1. (a) Optical images of porous $Ni(OH)_2$ films (right) and NiO films (left) prepared by mixed solvothermal method; inset shows that NiO on the back side had been removed completely. (b) Optical images of porous NiO films used to electrochemical test, with a film area of 2 cm×2 cm.
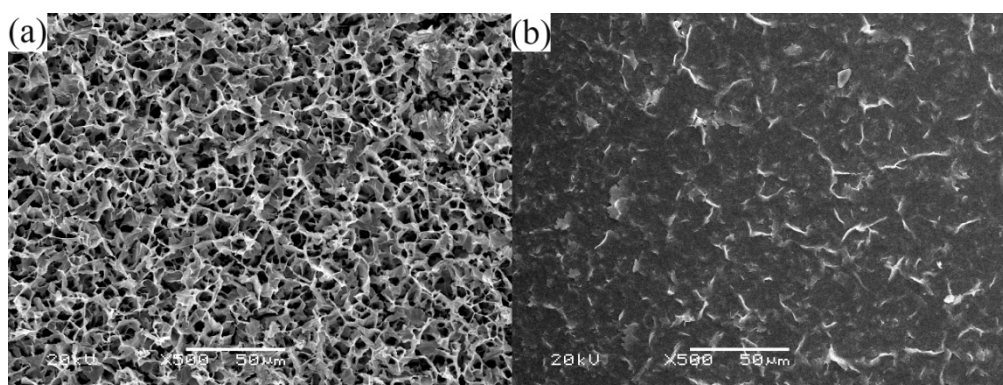

Figure S2. SEM images of porous NiO films prepared in the presence of glucose (a) and in the absence of glucose (b).
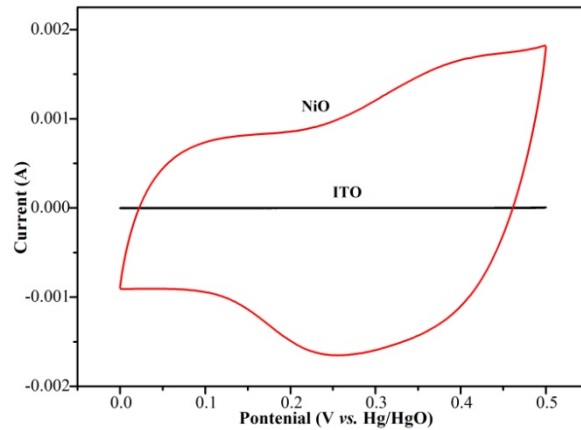
Figure S3. Cyclic voltammetry curves at a scan rate of 40 mV/s of the ITO (black) and porous NiO films (red) in 1 M KOH solution.
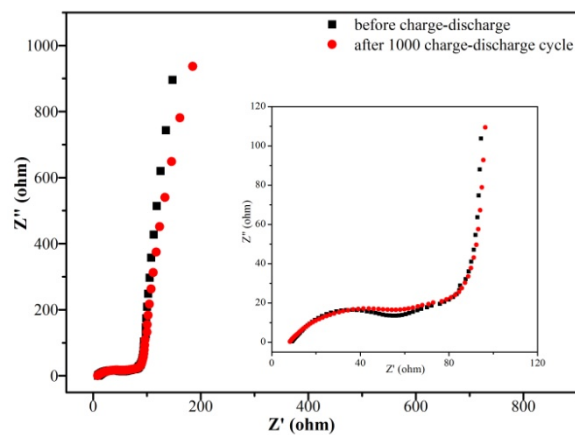

Figure S4. Nyquist plots of the porous NiO films electrode before and after charge-discharge cycling. Inset presents the magnified curves in high frequency regions.

Reference

1. G. Hu, C. Li, H. Gong, *J. Power Sources*, 2010, **195**, 6977.

2. C. Yuan, L. Yang, L. Hou, L. Shen, X. Zhang and X. W. Lou, *Energy Environ. Sci.*, 2012, **5**, 7883.

3. L.-B. Kong, M.-C. Liu, J.-W. Lang, M. Liu, Y.-C. Luo, L. Kang, *J. Solid State Electrochem.*, 2011, **15**, 71.

4. M. Kundu, L. Liu, *J. Power Sources*, 2013, **243**, 676.

5. D. P. Dubal, G. S. Gund, R. Holze, H. S. Jadhav, C. D. Lokhande and C.-J. Park, *Dalton Trans.*, 2013, **42**, 6459.

6. J. Zhu, L. Cao, Y. Wu, Y. Gong, Z. Liu, Ha. E. Hoster, Y. Zhang, S. Zhang, S. Yang, Q. Yan, P. M. Ajayan and R. Vajtai, *Nano Lett.*, 2013, *13*, 5408.

7 M. Yang, J. X. Li, H. H. Li, L.W. Su, J. P. Wei and Z. Zhou, *Phys. Chem. Chem. Phys.*, 2012, **14**, 11048.

9 H. W. Wang, H. Yi, X. Chen, X. F. Wang,, *Electrochim. Acta*, 2013, **105**, 353.

9 S. J. Ding , T. Zhu , J. S. Chen , Z. Y. Wang , C. L. Yuan , X. W. Lou, *J. Mater. Chem.*, 2011, **21**, 6602.

10 G. Q. Zhang, L. Yu, H. E. Hoster and X. W. Lou, *Nanoscale*, 2013, **5**, 877.

11 C.-Y. Cao, W. G., Z.-M. Cui, W.-G. Song and W. Cai, *J. Mater. Chem.*, 2011, **21**, 3204.

12 F. Lei, T. Le and G. Rong, *CrystEngComm*, 2011, **13**, 7246.

13 D. D. Han, P. C. Xu, X. Y. Jing, J. Wang, P. P. Yang, Q. H. Shen, J. Y. Liu, D. L. Song, Z. Gao, M. L. Zhang, *J. Power Sources*, 2013, **235**, 45.

14 H. Pang, Y. F. Shi, J. M. Du, Y. H. Ma, G. C. Li, J. Chen, J. S. Zhang, H. H. Zheng, B. Q. Yuan, *Electrochim. Acta*, 2012, **85**, 256.

15 X. Sun, G. K. Wang, J.-Y. Hwang and J. Lian, *J. Mater. Chem.*, 2011, 21, 16581.

16 C. Z. Yuan, X. G. Zhang, L. H. Su, B. Gao and L. F. Shen, *J. Mater. Chem.*, 2009, **19**, 5772.

17 B. Wang, J. S. Chen, Z. Wang, S. Madhavi and X. W. Lou, *Adv. Energy Mater.*, 2012, **2**, 1188.

18 J. H. Zhu, J. Jiang, J. P. Liu, R. M. Ding, H. Ding, Y. M. Feng, G. M. Wei, X. T. Huang, *J. Solid State Chem.*, 2011, **184**, 578.

19 C. Z. Yuan, J. Y. Li, L. R. Hou, L. Yang, L. F. Shen, X. G. Zhang, *Electrochim. Acta*, 2012, **78**, 532.

20 X. L. Li, S. L. Xiong, J. F. Li, J. Bai and Y. T. Qian, *J. Mater. Chem.*, 2012, **22**, 14276.